ChemComm

COMMUNICATION

View Article Online
View Journal | View Issue

Cite this: *Chem. Commun.*, 2022, **58**, 7690

Received 16th May 2022,
Accepted 10th June 2022

DOI: 10.1039/d2cc02782h

rsc.li/chemcomm

Modulating the antibacterial activity of gold nanoparticles by balancing their monodispersity and aggregation†

Le Wang,‡[a] Wenfu Zheng,‡[b] Sixiang Li,[a] Qinghong Hou[a] and Xingyu Jiang *[a]

Aggregation is a key factor influencing the function of nanoparticles. Thioproline-modified gold nanoparticles show potent antibacterial activity, which is compromised by thioproline-mediated particle aggregation. By tuning the balance between the exposure and shielding of thioproline, a maximal antibacterial property of the gold nanoparticles is achieved.

Recently, nanomaterials have received considerable attention owing to their specific physicochemical properties, such as high specific surface area,[1–3] tunable size and shape,[4–7] and multiple modification strategies for applications in various fields.[8–10] Monodispersity is a prerequisite to maintain the specific properties of the nanomaterials. To prevent the particle aggregation, researchers have used various methods such as the change of the solvent, the addition of dispersants and pH value adjustment.[11–13] However, these methods may affect the original properties of the nanoparticles and hinder their applications. Thus, new strategies that can simultaneously optimize the particle function and maintain an ideal monodispersity of the nanomaterials are highly desirable, particularly for biomedical applications.[14–17]

L-thioproline (T) is not only an anti-tumor drug[18,19] but also a starting material for synthesizing pidotimod, an immunomodulator.[20–24] Thus, thioproline is an ideal candidate for activating gold nanomaterials since an essential requirement of antibiotics is that they are nontoxic to human cells. Here, we use T to modify gold nanoparticles (T-Au NPs) to explore their antibacterial activity. The starting materials (T and Au NPs) of the T-Au NPs have a low toxicity profile. However, the T-Au NPs tend to aggregate in the physiological environment, which greatly hampers their antibacterial efficiency. To achieve monodispersion of the nanoparticles, we use Boc-protected thioproline (B) to modify the Au NPs (B-Au NPs). The resulting B-Au NPs, although show good dispersity, display compromised antibacterial efficacy, demonstrating that the exposure of an active group of the T is necessary for maintaining the antibacterial activity of the Au NPs. To attain an optimized antibacterial effect, we present a strategy to co-modify T and B on Au NPs (TB-Au NPs) with various molecular ratios. We find that when the ratio of T and B is 1 : 1, the corresponding TB-Au NPs (T_1B_1-Au NPs) have the optimized antibacterial performance (Scheme 1).

We successfully synthesize T-Au NPs by a one-step reduction method. The T-Au NPs appear as aggregated small nanoparticles with an average diameter of 51.1 ± 3.0 nm under transmission electron microscopy (TEM) and an average diameter of 71.4 nm under dynamic light scattering (DLS) (Fig. 1). The shape of the single T-Au NPs is spherical, but the intermolecular bonding between the amino groups and the carboxyl groups causes the aggregation of the particles. Sulfydryl (–SH) exhibits stronger bonds with gold than amino ($–NH_2$),[25–27] so T anchors Au NPs mainly by –SH, while the amino and carboxyl groups on T are exposed, which may mediate the

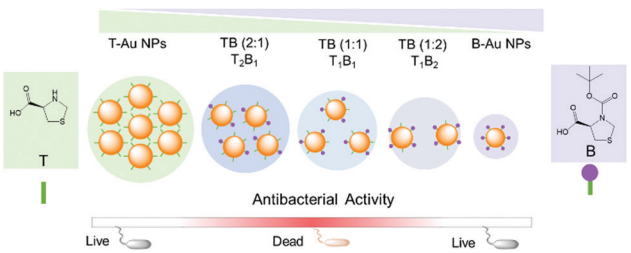

Scheme 1 Schematic illustration of the synthesis strategy of TB-Au NPs to tune their antibacterial efficacy.

[a] *Guangdong Provincial Key Laboratory of Advanced Biomaterials, Shenzhen Key Laboratory of Smart Healthcare Engineering, Department of Biomedical Engineering, Southern University of Science and Technology, No. 1088 Xueyuan Rd, Nanshan District, Shenzhen, Guangdong, 518055, China. E-mail: jiang@sustech.edu.cn*

[b] *GBA Research Innovation Institute for Nanotechnology, CAS Key Lab for Biological Effects of Nanomaterials and Nanosafety, National Center for NanoScience and Technology, No. 11 Zhongguancun Beiyitiao, Beijing, 100190, China*

† Electronic supplementary information (ESI) available. See DOI: https://doi.org/10.1039/d2cc02782h

‡ These authors contributed equally.

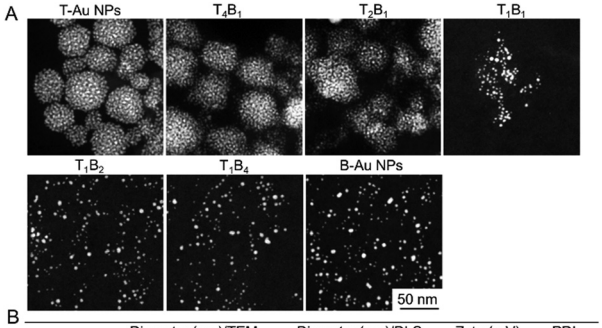

B

	Diameter (nm)/TEM	Diameter (nm)/DLS	Zeta (mV)	PDI
T-Au NPs	51.1 ± 3.0	71.4	-37.2	0.263
T_4B_1	45.6 ± 1.4	63.8	-22.0	0.219
T_2B_1	39.7 ± 3.2	52.9	-14.2	0.372
T_1B_1	21.7 ± 2.8	40.5	-13.7	0.295
T_1B_2	3.8 ± 0.5	22.6	-7.4	0.394
T_1B_4	2.3 ± 0.2	19.2	-9.1	0.284
B-Au NPs	2.4 ± 0.1	13.8	-8.9	0.317

Fig. 1 Characterization of T-Au NPs, B-Au NPs and TB-Au NPs. (A) TEM images of T-Au NPs, B-Au NPs, and TB-Au NPs with different T/B ratios. (B) Average diameter and Zeta potential of the T-Au NPs, B-Au NPs, and TB-Au NPs with different T/B ratios.

intermolecular interactions and lead to the aggregation between the nanoparticles. The aggregation of the T-Au NPs will inevitably lead to shielding effects for the active groups of the T and the compromising of the antibacterial efficacy of the nanoparticles. We attempt to synthesize the T-Au NPs under different pH conditions to avoid the aggregation. After adjusting the pH value of the synthetic conditions by adding acid (acetic acid) or alkali (sodium hydroxide), the resulting T-Au NPs still have an aggregated appearance (ESI,† Fig. S1).

Inspired by the strategy that during the synthesis of peptides, protecting groups are often introduced to shield some groups of the substrate molecules to control the synthesis process, we select B as an alternative molecule to modify the Au NPs to avoid particle aggregation. We measure the minimal inhibition concentration (MIC) of the bare Au NPs, T, and B, respectively. Even at a high concentration (128 μg mL^{-1}), the bare Au NPs, T, or B show no antibacterial effect by themselves (Table S1, ESI†). As expected, the resulting B-Au NPs display monodispersity with an average diameter of 2.4 ± 0.1 nm under TEM and 13.8 nm under DLS (Fig. 1). However, the antibacterial efficacy of the B-Au NPs is significantly lower than that of the T-Au NPs (Table 1), demonstrating that the Boc cap shields the active groups of the T and compromises the antibacterial efficacy of the resulting nanoparticles.

To exclude the possible influence of the Boc group on the dispersity and the antibacterial activity of the Au NPs, we utilize another protecting group, acetyl, to cap the thioproline. We synthesize acetyl-thiazolidine (Mw = 175.206)-modified gold nanoparticles (A-Au NPs) by a one-step reduction method. The average diameter and the Zeta potential of the A-Au NPs are 6.4 ± 1.4 nm and −27.4 mV, respectively (Table S2, ESI†). DLS curves indicate that there is no significant aggregation in the particle solution (Fig. S2, ESI†). The MIC of A-Au NPs against *E. coli* and multidrug resistant (MDR) *E. coli* is over 64 μg mL^{-1}, demonstrating a low antibacterial activity

Table 1 MIC (μg mL^{-1}) of different Au NPs and antibiotics against Gram-negative bacteria. The MIC of TB-Au NPs is the sum of the mass of the gold core and surface ligands, so it is not an integer value

MIC (μg mL^{-1})	*E. coli*	*P.a*	*K.p*	*A.b*	MDR *E. coli*	MDR *P.a*	MDR *K.p*	MDR *A.b*
T-Au NPs	28.7	57.4	28.7	28.7	28.7	14.4	28.7	57.4
T_4B_1	14.5	29.0	14.5	29.0	14.5	14.5	29.0	58.0
T_2B_1	11.7	23.4	11.7	23.4	11.7	5.9	23.4	23.4
T_1B_1	4.8	9.6	4.8	9.6	4.8	4.8	9.6	19.2
T_1B_2	4.9	9.8	4.9	9.8	9.8	4.9	9.8	19.6
T_1B_4	5.1	10.1	10.1	10.1	10.1	10.1	20.2	20.2
B-Au NPs	39.8	79.6	19.9	39.8	39.8	19.9	39.8	79.6
Polymyxin B	1	2	1	8	1	128	1	2
Gentamicin	4	2	1	8	128	64	128	128
Ampicillin	8	128	32	32	128	128	128	128

(Table S3, ESI†). The results indicate that the capping of the amino group can indeed avoid the particle aggregation and simultaneously decrease the antibacterial activity of the T-Au NPs, highlighting the role of the amino group on the Au NPs.

We explore if the deprotection of Boc-protected thioproline on the B-Au NPs can expose active sites to improve the antibacterial activity of the nanoparticles and avoid the aggregation of the nanoparticles. We use hydrochloric acid (HCl) or trifluoroacetic acid (TFA) to remove the Boc group. After the reaction, the Au NPs aggregate to different extents (Fig. 2A and B). The Zeta potentials of the deprotected Au NPs are close to that of the T-Au NPs (−37.2 mV), indicating the successful removal of the Boc groups and the change of the B-Au NPs to T-Au NPs (Table S4, ESI†). The carboxyl group on the T may dominate the surface potential of the Au NPs, thus, after deprotecting the Boc group with HCl and TFA, the resulting T-Au NPs still keep a negative Zeta potential. The MIC of the deprotected Au NPs exhibits no significant change (Table S5, ESI†). Thus, the exposure of active sites of the T by deprotection of Boc can cause the aggregation of the nanoparticles and cannot improve their antibacterial activity. We synthesize Au

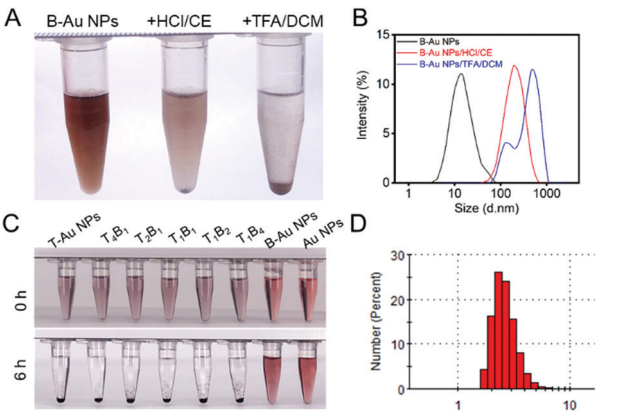

Fig. 2 Characterization of B-Au NPs after Boc deprotection by different methods. (A) Photos of B-Au NPs and the resulting deprotected Au NPs. (B) DLS analysis of B-Au NPs and the resulting deprotected Au NPs. (C) Images of T-Au NPs, B-Au NPs, and TB-Au NPs with different T/B ratios synthesized with a ligand exchange reaction. (D) Average diameter of Au NPs tested by DLS.

NPs (Fig. 2C and D) and cap T or B on the Au NPs by ligands exchange reactions. Still, the Au NPs aggregate to different extents and the stability of these TB-Au NPs is poor (Fig. 2C and D), which is not suitable for the antibacterial test.

To optimize the antibacterial property of the Au NPs, a balance between the particle aggregation and the exposure of the active groups on the T should be achieved. So we attempt to co-modify the Au NPs with T and B with different molecular ratios (T : B from 4 : 1, 2 : 1, 1 : 1, 1 : 2 to 1 : 4) and evaluate the changes in the characterizations of the yielding nanoparticles (TB-Au NPs). With the increase of the ratio of B, the aggregation of TB-Au NPs is significantly reduced and the average diameter of the particles decrease from 51.1 nm (T-Au NPs) to 2.3 nm (T : B = 1 : 4, T_1B_4) under TEM, which is consistent with the result of the DLS. With the increase of the ratio of B, the dispersity of TB-Au NPs is significantly improved (Fig. 1A). We measure the UV-vis absorbance spectra of different Au NPs. The adsorption peaks of the Au NPs are around 520 nm, which is the typical surface plasmon resonance of Au NPs (Fig. S3, ESI†). The characteristic plasmonic absorption peak of gold is weakened due to the aggregation or small particle size. Generally, Au NPs smaller than 3 nm do not have conspicuous peaks.[28,29] All the Au NPs are negatively charged in the solution, and as the ratio of B : T increases, the absolute value of the Zeta potential of the TB-Au NPs decreases from −37.2 to −8.9 mV (Fig. 1B).

We use X-ray photoelectron spectroscopy (XPS) to test the ratio of sulfur (unique element of T or B) to gold (Au) and calculate the number of molecules on each Au NPs (Table S6, ESI†). We explore the MIC of TB-Au NPs with different T/B ratios against Gram-negative bacteria, including the antibiotic-sensitive strains and their corresponding MDR strains. For T_1B_4-Au NPs, although they have a smaller size than the T_1B_1-Au NPs, most of their exposed molecule is B, which covers the active groups on T. When the ratio of T and B is 1 : 1 (T_1B_1), a balance between the particle aggregation and the exposure of the active groups on the T is achieved, so they have the best antibacterial performance, and we select T_1B_1-Au NPs to carry out the following experiments. The bare Au NPs, T, and B show no antibacterial activity. After T and B modification, the resulting TB-Au NPs have potent antibacterial activity (Fig. 3). This means that T endows the Au NPs with antibacterial activity. T has an amino and a sulfhydryl group, which can bind to the Au NPs (mainly by sulfhydryl group) and attach to bacteria (mainly by amino group), respectively. The MIC of T_1B_1-Au NPs can be less than 4.8 μg mL^{-1} even for the MDR bacteria (Table 1). Thus, the TB-Au NPs with appropriate T/B ratios could fight against the MDR bacteria, which are challenging for clinical antibiotics.

We evaluate the morphological change of different Gram-negative bacteria treated by T_1B_1-Au NPs by scanning electron microscopy (SEM). After T_1B_1-Au NP treatment, the bacteria merge together and the cell wall structure collapses apparently, indicating the significant bacteria disruption (Fig. 3A). Compared with the control bacteria with an intact cell wall, the cell wall structure of the T_1B_1-Au NP-treated (8 μg mL^{-1}) bacteria becomes blurred (Fig. 3B). As the concentration of T_1B_1-Au NPs increases (16 μg mL^{-1}), the cell wall of the treated bacteria ruptures completely and the bacterial lysis is significant (Fig. 3B). We stain bacteria (*P.a*, MDR *P.a*) with SYTO9/PI to investigate the permeability changes of the bacterial cell membrane in the presence of the T_1B_1-Au NPs. The bacterial cells treated with T_1B_1-Au NPs show sharp membrane damage (Fig. S4, ESI†). Hence, T_1B_1-Au NPs can induce the increase of the cell membrane permeability to kill the bacteria. Although the negative charge of T_1B_1-Au NPs may hinder their interaction with the negatively charged bacteria, the carboxylic acid groups of T ligands can compete for the hydrogen bonding interactions with lipopolysaccharides/peptidoglycans on the surface of bacteria.[30,31] This process may lead to the disruption of the hydrogen bonding within the cell wall and cause the instability and rupture of the cell wall structure, which is a possible mechanism for the antibacterial activity of T_1B_1-Au NPs.

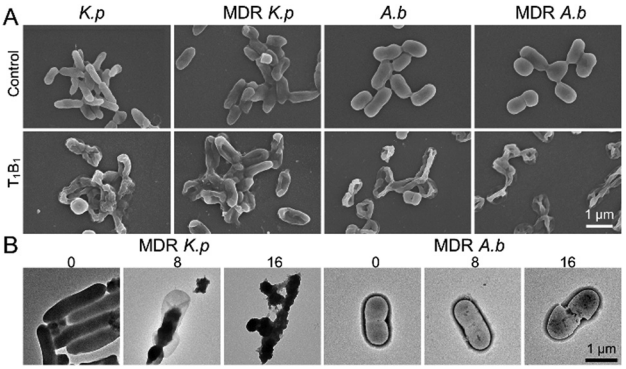

Fig. 3 The antibacterial effect of T_1B_1-Au NPs on different bacteria *in vitro*. (A) SEM images and (B) TEM images of the bacteria treated with T_1B_1-Au NPs. Scale bars, 1 μm.

We evaluate the biocompatibility of T_1B_1-Au NPs because the biological safety is a critical property of the biomaterials in further clinical applications. Human fibroblast (HAF) cells treated with T_1B_1-Au NPs show intact morphology and good proliferative conditions, indicating that the Au NPs have no cytotoxicity (Fig. 4A). The cell viability of human umbilical vascular endothelial cells (HUVECs) treated by different concentrations of T_1B_1-Au NPs is similar to those in the control group ($P > 0.05$, *t*-test, Fig. 4B), indicating that T_1B_1-Au NPs could serve as a safe agent for mammalian cells. Compared with the control group, the cell density treated by T_1B_1-Au NPs shows no significant decrease for different incubation times ($P > 0.05$, *t*-test, 24 h and 48 h), which means that the T_1B_1-Au NPs could not block the proliferation of the HUVECs (Fig. 4C). We also evaluate the toxicity of the starting materials (T, B and Au NPs) on HUVECs. Even when the concentration of starting materials increases to 64 μg mL^{-1}, the cell viability is still higher than 85% (Fig. S5A, ESI†), indicating that the starting materials are safe for the mammalian cells. Moreover, the morphology and cell number of HAFs cultured with the starting materials (concentration, 64 μg mL^{-1}, 48 h) are similar to those of the control group (Fig. S5B, ESI†), indicating that T, B and Au NPs have negligible adverse effects on cell viability and proliferation.

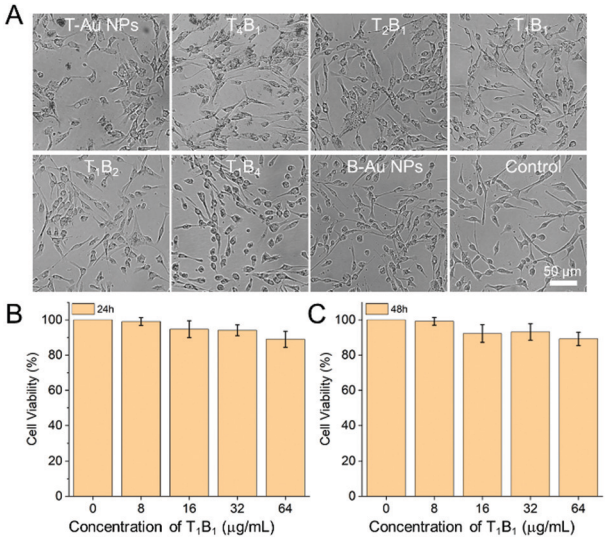

Fig. 4 Biocompatibility of the T-Au NPs, B-Au NPs, and TB-Au NPs with different T/B ratios. (A) Morphologies of HAF incubated with various Au NPs. Scale bars, 50 μm. (B and C) Cytotoxicity evaluation of HUVECs treated by various concentrations of T_1B_1-Au NPs.

In this study, we use a chemical protecting group commonly used in organic reactions, Boc, to modulate the aggregation of Au NPs to achieve a maximal antibacterial property of the nanoparticles. The protection group strategy is thus insightful for exploring the potential of many existing nanomaterials or nanosystems which face the problem of particle aggregation. We believe that this strategy can dramatically open up the potential applications of many types of nanoparticles that are hard to disperse in aqueous solutions. Moreover, other issues such as the toxicity of nanomaterials may be overcome by replacing or shielding certain groups on the nanomaterials while still retaining or even enhancing their biochemical functions. This strategy could also be extended to other fields such as the shielding of foreign groups to avoid immunological attack and spatiotemporally controlled drug release.

Le Wang, Wenfu Zheng, and Xingyu Jiang designed the experiment, Le Wang, Qinghong Hou, and Sixiang Li performed the experiments. Le Wang, Wenfu Zheng, and Xingyu Jiang analyzed the data and wrote the manuscript. Xingyu Jiang supervised the whole project.

We thank the National Key R&D Program of China (2018YFA0902600), the National Natural Science Foundation of China (81730051 and 32071390), the Shenzhen Science and Technology Program (KQTD20190929172743294), the Guangdong Provincial Key Laboratory of Advanced Biomaterials (2022B1212010003), the Shenzhen Key Laboratory of Smart Healthcare Engineering (ZDSYS20200811144003009), the Guangdong Innovative and Entrepreneurial Research Team Program (2019ZT08Y191), and the Tencent Foundation through the XPLORER PRIZE for financial support. The authors acknowledge the assistance of SUSTech Core Research Facilities.

Conflicts of interest

There are no conflicts of interest to declare.

Notes and references

1 V. Montes-Garcia, M. A. Squillaci, M. Diez-Castellnou, Q. K. Ong, F. Stellacci and P. Samori, *Chem. Soc. Rev.*, 2021, **50**, 1269.
2 M. Azharuddin, G. H. Zhu, D. Das, E. Ozgur, L. Uzun, A. P. F. Turner and H. K. Patra, *Chem. Commun.*, 2019, **55**, 6964.
3 J. Mao, Y. Chen, J. Pei, D. Wang and Y. Li, *Chem. Commun.*, 2016, **52**, 5985.
4 Y. Wang, Y. Jin, W. Chen, J. Wang, H. Chen, L. Sun, X. Li, J. Ji, Q. Yu, L. Shen and B. Wang, *Chem. Eng. J.*, 2019, **358**, 74.
5 L. Wang, W. Zheng, L. Zhong, Y. Yang, S. Li, Q. Li and X. Jiang, *Chem. Commun.*, 2022, **58**, 2842.
6 P. Gao, R. Wei, B. Cui, X. Liu, Y. Chen, W. Pan, N. Li and B. Tang, *Chem. Commun.*, 2021, **57**, 6082.
7 Y. Hou, Y. Liu, C. Tang, Y. Tan, X. Zheng, Y. Deng, N. He and S. Li, *Chem. Eng. J.*, 2022, **435**, 134145.
8 Y. Cao, J. Wu, B. Pang, H. Zhang and X. C. Le, *Chem. Commun.*, 2021, **57**, 6871.
9 Y. Zhang, B. Y. W. Hsu, C. Ren, X. Li and J. Wang, *Chem. Soc. Rev.*, 2015, **44**, 315.
10 J. Lin, J. Li, A. Gopal, T. Munshi, Y. Chu, J. Wang, T. Liu, B. Shi, X. Chen and L. Yan, *Chem. Commun.*, 2019, **55**, 2656.
11 Z. Huang, B. Liu and J. Liu, *Nanoscale*, 2020, **12**, 22467.
12 T. Shu, L. Su, J. Wang, X. Lu, F. Liang, C. Li and X. Zhang, *Anal. Chem.*, 2016, **88**, 6071.
13 C. Xiang, F. Yang, M. Li, M. Jaridi and N. Wu, *J. Nanopart. Res.*, 2012, **15**, 1293.
14 X. Huang, H. Liang, Z. Li, J. Zhou, X. Chen, S. Bai and H. Yang, *Nanoscale*, 2017, **9**, 2695.
15 E. C. Dreaden, A. M. Alkilany, X. Huang, C. J. Murphy and M. A. El-Sayed, *Chem. Soc. Rev.*, 2012, **41**, 2740.
16 H. Huang, W. Feng and Y. Chen, *Chem. Soc. Rev.*, 2021, **50**, 11381.
17 Y. G. Srinivasulu, Q. Yao, N. Goswami and J. Xie, *Mater. Horiz.*, 2020, **7**, 2596.
18 M. Charehsaz, F. Onen-Bayram, H. Sipahi, K. Buran, A. Giri and A. Aydin, *Exp. Toxicol.*, 2016, **35**, 1108.
19 S. H. Kim, H. J. Kim and H. S. Shin, *J. Pharm. Biomed. Anal.*, 2014, **100**, 58.
20 M. Sara, F. P. Giuseppe, P. Maria and L. Salvatore, *Minerva Pediatr.*, 2020, **72**, 358.
21 S. Esposito, M. Garziano, V. Rainone, D. Trabattoni, M. Biasin, L. Senatore, P. Marchisio, M. Rossi, N. Principi and M. Clerici, *J. Transl. Med.*, 2015, **13**, 288.
22 D. Gourgiotis, N. G. Papadopoulos, A. Bossios, P. Zamanis and P. Saxoni, *J. Asthma*, 2004, **41**, 285.
23 G. V. Zuccotti and C. Mameli, *Ital. J. Pediatr.*, 2013, **39**, 75.
24 S. Hu, X. Fu, A. Fu, W. Du, J. Ji and W. Li, *Amino Acids*, 2014, **46**, 1177.
25 F. Chen, X. L. Li, J. Hihath, Z. F. Huang and N. J. Tao, *J. Am. Chem. Soc.*, 2006, **128**, 15874.
26 L. Wang, S. Li, J. Yin, J. Yang, Q. Li, W. Zheng, S. Liu and X. Jiang, *Nano Lett.*, 2020, **20**, 5036.
27 E. Podstawka, Y. Ozaki and L. M. Proniewicz, *Appl. Spectrosc.*, 2005, **59**, 1516.
28 H. Koerner, R. I. MacCuspie, K. Park and R. A. Vaia, *Chem. Mater.*, 2012, **24**, 981.
29 M. J. Hostetler, J. E. Wingate, C. Zhong, J. E. Harris, R. W. Vachet, M. R. Clark, J. D. Londono, S. J. Green, J. J. Stokes and G. D. Wignall, *Langmuir*, 1998, **14**, 17.
30 P. P. Pillai, B. Kowalczyk, K. Kandere-Grzybowska, M. Borkowska and B. A. Grzybowski, *Angew. Chem., Int. Ed.*, 2016, **128**, 8752.
31 C. R. H. Raetz and C. Whitfield, *Annu. Rev. Biochem.*, 2002, **71** 635.